

Electrohydrodynamic and Aerosol Jet Printing for the Copatterning of Polydimethylsiloxane and Graphene Platelet Inks

Nathan J. Wilkinson, Robert W. Kay, and Russell A. Harris*

The performance of soft sensing and actuation devices is dependent on their design, the electro-mechanical response of materials, and the ability to copattern structural and functional features. For film based soft structures, such as wearable sensors and artificial muscles, manufacturing challenges exist that prevent the translation of technology from laboratory to practical application. In this work, a hybrid manufacturing technique is presented that integrates electro-hydrodynamic and aerosol jet deposition to print multilayer, multimaterial structures. The combined approach overcomes the respective rheological constraints of the individual processes, while presenting a pathway to higher resolution computer-controlled patterning. Electro-hydrodynamic deposition of a polydimethylsiloxane elastomer is demonstrated and characterized, before being combined with aerosol jet deposition of a graphene platelet ink to produce functional devices. A proof-of-concept, multilayer capacitive sensor is presented as a first demonstration of the manufacturing technology.

Soft robotics presents a unique opportunity to improve the interactions and interfaces between living and computerized systems to drive innovation in healthcare,^[1] haptics,^[2] and biological sciences.^[3] Film-based soft robotics, in the form of actuators and sensors, are of interest due their low-weight, high efficiency, and unobtrusive nature.^[4] Innovation in their manufacture, to allow selective patterning of soft and functional materials at improved resolution, will be essential to delivering the potential of soft technologies and will drive their commercial adoption.^[5] Specifically, the ability to alternately form thin layers of elastomers with micro-patterned, stretchable circuitry can improve sensor density and fidelity. The automated and repeatable manufacture of low-roughness elastomeric films has importance in actuation technologies as it is the key enabler for dielectric electroactive polymers, commonly known as a type of artificial muscle.^[6]

N. J. Wilkinson, Dr. R. W. Kay, Prof. R. A. Harris
Future Manufacturing Processes Research Group
University of Leeds
Leeds LS2 9JT, UK
E-mail: R.Harris@leeds.ac.uk

 The ORCID identification number(s) for the author(s) of this article can be found under <https://doi.org/10.1002/admt.202000148>.

© 2020 The Authors. Published by WILEY-VCH Verlag GmbH & Co. KGaA, Weinheim. This is an open access article under the terms of the Creative Commons Attribution License, which permits use, distribution and reproduction in any medium, provided the original work is properly cited.

DOI: 10.1002/admt.202000148

Several techniques have been developed for film based soft robotic devices, but they face challenges in processing speed, scalability, and resolution. Common approaches use spin coating,^[7,8] blade casting,^[9] or pad printing^[10] to produce thin layers of elastomer often in combination with masked deposition of electrodes. Despite some success, film thicknesses below 5 μm are challenging and there are limits to the height and area of stacked elastomer structures.^[11] Furthermore, these batch processes do not provide opportunity for patterning of elastomer layers and face challenges at larger volumes.

Additive techniques, which selectively deposit elastomeric and functional materials, are removing design constraints and offering new capabilities through improved design. The disparity in rheology between functional and structural inks provides the most prominent hurdle to the development of an effective and integrated manufacturing strategy. Direct ink write (DIW) is growing in popularity for soft robotics,^[12] however the process resolution is better suited for large devices over film-based sensors or actuators. Ink jet printing has been the most successful for thin films, with McCoul et al.^[13] demonstrating the deposition of thin (2–5 μm) elastomer layers. The authors maintained that nozzle clogging is a significant issue even when using relatively large nozzle orifices with diluted inks. The aforementioned techniques have been most successful in the patterning of functional materials within soft structures. DIW,^[14] aerosol jet (AJ),^[15] and inkjet printing^[16] have all been demonstrated as effective methods for producing stretchable or flexible sensors and actuators.

Electro-hydrodynamic Jet (E-Jet) printing—an additive technique that uses high electric fields to draw material from a nozzle—has been widely investigated for its ability to deposit sub-micron features.^[17] Since material is drawn rather than pushed through the application of back-pressure, E-Jet deposition is also able to deposit higher viscosity materials than comparable processes.^[18] In this work, we leverage this improved material compatibility through a non-classical deposition regime to selectively pattern unmodified, commercially available polydimethylsiloxane (PDMS). Pulsating jet and pulse-on-demand droplet deposition is investigated before being combined with oxygen plasma surface treatment and AJ printing to demonstrate a digitally driven process route for the

hybrid manufacture of a functional multilayer, multimaterial structure.

When a volume of liquid is ejected from a nozzle, a spheroidal meniscus forms as the surface tension of the fluid is the principle force dictating its shape. Under a high electric field, stresses driven by charge interactions become the predominant factor and, beyond a critical value, the electric field will pull the meniscus in to a conical structure that emits a jet from its apex.^[19] If the substrate is sufficiently close to the nozzle, the jet can be used for direct write (E-Jet) before whipping^[20] or spraying^[21] instabilities arise.

Establishing classical electro-hydrodynamic deposition requires the fluid's electrical relaxation time to be shorter than the hydrodynamic relaxation time^[22] (Equation (1)), where ϵ' is the permittivity of the fluid, ϵ_0 is the permittivity of free space, K is the conductivity of the ink, L is the distance between the nozzle and electrode, D is the nozzle diameter, and Q_s is the supplied flow rate

$$\frac{\epsilon' \epsilon_0}{K} \ll \frac{LD^2}{Q_s} \quad (1)$$

Deposition of silicone elastomers, or silicone oils,^[23] through the classical regime can be a challenge due to their low-conductivity. Existing work targeting electro-hydrodynamic deposition of PDMS has modified the ink through simplification of the precursor solution,^[24] using carrier materials within the solution,^[25] or some combination of the two.^[11] These methods aim to increase the conductivity and reduce the permittivity of the fluid to increase the material's affinity to classical deposition.

When the material's electrical relaxation time exceeds the hydrodynamic time, an alternate deposition mechanism known as electrically forced jets arises.^[22] In practice, this leads to a loss of resolution compared to classical E-Jet due to the establishment of a ball-cone rather than the traditional Taylor cone. For many soft film applications, increased lateral resolution may present a suitable compromise for increased material compatibility, especially if axial resolution can be preserved. In this study, we investigate the production of droplets through electrically forced jets and the effect of processing parameters on the shape and size of the deposits.

Droplet production can be triggered through the pulsating jet or drop-on-demand techniques. In the pulsating mode, ejection is a result of cyclic imbalances between the surface tension and electrostatic stresses within the meniscus under the application of a static DC field. Once the electrostatic stresses overcome the surface tension, a droplet is ejected and the cone recoils. The process then repeats at high frequencies to produce a steady stream of droplets. The frequency of droplet emission is driven by the properties of the ink, such as viscosity and conductivity, in combination with the applied voltage, nozzle-substrate distance, and material flowrate (Figure 1a).

Increasing the magnitude of the DC electric field, through either an increase in the applied voltage or reduction of the nozzle-substrate offset, increases the frequency of the droplet emission and reduces the size of the droplets. Increasing the flow rate led to increased droplet size and a reduction in droplet frequency. The close coupling between process control,

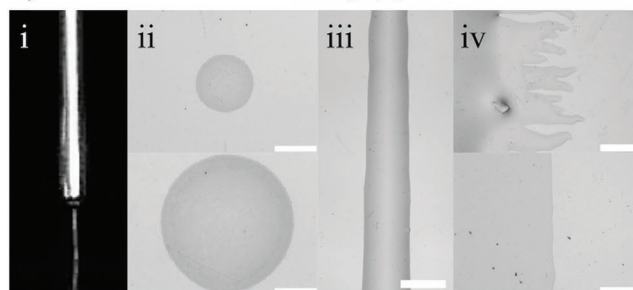
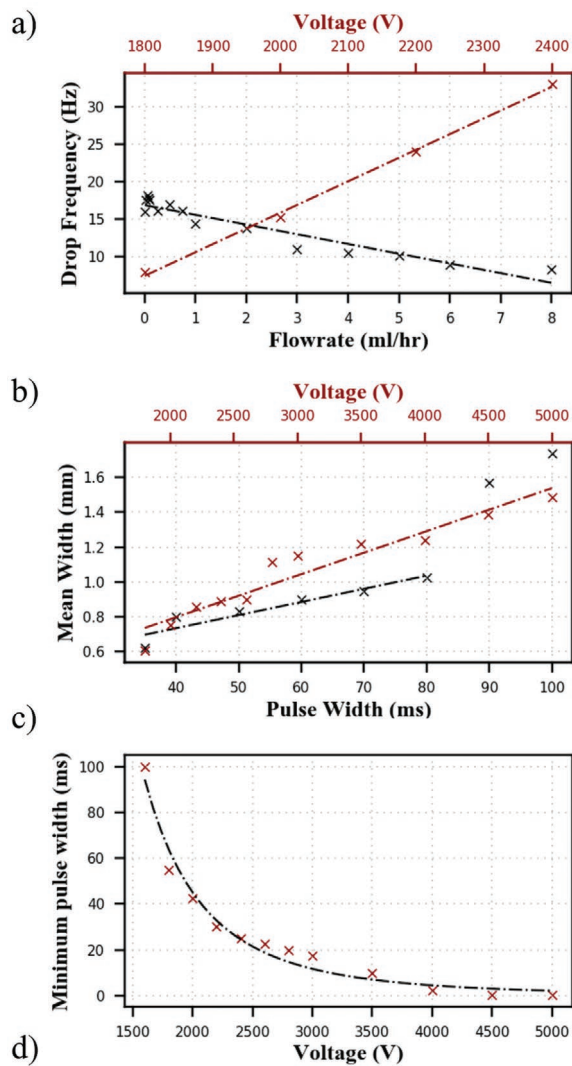


Figure 1. a) Effect of flowrate and applied voltage on droplet frequency in the pulsating jet mode, b) the effect of increasing high voltage pulse width and magnitude on the droplet width, c) Minimum pulse width required to trigger deposition at increasing voltages, d) Micrographs of i) droplet ejection, ii) droplets at the minimum and maximum pulse widths, iii) a confluent line, iv) effects of DC versus AC pulses during pulse-on-demand deposition. All scale bars are 500 μm

droplet size, and frequency provided limited spatial control and resulted in the spacing between consecutive droplets being driven by the translational velocity of the deposition head. This approach requires significant empirical work to understand the interdependencies and derive a reliable process.

Pulse-on-demand differs as it selectively applies a high voltage pulse to trigger droplet ejection. This provides simplified, independent control of droplet volume and positioning. Decreasing the magnitude and duration of the applied pulse allows a reduction in deposit diameter (Figure 1b), while spatial control can be achieved through coordination of the deposition head with the application of the pulse. For the materials used in this work, high magnitude pulses in combination with short pulse durations were found to be an effective method to increase droplet throughput (Figure 1c), even at voltages that were found to produce unstable jetting in a static field.

In contrast to pulsating E-Jet, increasing the magnitude of the applied voltage pulse was found to increase the diameter of the deposit (Figure 1b). When observed using stroboscopic microscopy, ejection of multiple droplets were identified during the application of a 100 ms square-wave pulse. As shown in Figure 1b, the discontinuity in the pulse width represents the pulse duration required to trigger multiple droplets under a 2 kV electric field.

Deposit geometry was controlled through modulation of the applied voltage and pulse-width. Adjustment of the nozzle-substrate distance allows similar control, however reducing the nozzle offset was found to increase the variation in droplet size. This behaviour is likely due to reduced variation in the magnitude of the electric field caused by misalignments in the motion platform. Deposition at offsets of 3 mm allowed consistent deposition without excessive voltage requirements.

The limited spatial resolution (minimum deposit diameter $\approx 500 \mu\text{m}$) can be attributed to both the nozzle size (160 μm ID) and spreading of the elastomer when it impacts the surface. The contact angle between the elastomer drop and the substrate was found to be 1.2° degrees (Figure S1, Supporting Information). The minimum volume of the droplets presented here are estimated to be $\approx 800 \text{ pL}$ by assuming constant volume during deposition and curing. Although larger than traditional inkjet printing processes, this represents a significant increase over minimum volume when compared to DIW.^[26] Furthermore, since no significant instances of nozzle blocking occurred, this could likely be reduced with smaller nozzles in subsequent studies; however, for the film-based devices targeted in this work, the trade-off between manufacturing speed and resolution needs to be considered.

Reducing the spacing between consecutive droplets allows the production of confluent features. A droplet overlap of approximately 40% (Figure S2, Supporting Information) represented a suitable balance when trying to maintain line width and height, while minimizing the gaps within the films. Ejecting droplets in close proximity under a DC field led to charge repulsion in the deposit when attempting to produce films. This manifested itself in the production of dendrites or fingers that reduced edge resolution (Figure 1div). By switching the polarity of consecutive pulses, charge accumulation was avoided and edge definition improved. The polarity of the applied pulse was found to have minimal effect on droplet volume (Figure S3, Supporting Information) when compared to the magnitude.

Patterning multiple inks to produce more functional devices can introduce challenges caused by the interactions of materials. The low porosity and surface energy of PDMS, coupled

with the relatively high surface tension of aqueous inks, often leads to limited material wetting and adhesion. These hurdles are more apparent for conductive inks where additives to promote adhesion can have a detrimental effect on the functionality of the deposit.

To encourage adhesion, spreading, and the production of confluent features, PDMS was exposed to an oxygen plasma surface treatment to increase the surface energy of the substrate. The sessile drop imaging technique was used to provide an indication of the efficacy of the plasma treatment and to understand the effect of exposure time on material wetting. An exposure time of six seconds was used to treat the PDMS samples since further exposure had minimal effect on the contact angle and excessive exposure can lead to surface oxidation.

AJ printing is a contactless deposition technique originally developed for the deposition of high-resolution conductive circuitry. Recent reviews of the technique have focused on the underlying deposition mechanism^[27] and applications of the process.^[28] In this work the process is used to provide reliable, selective patterning of a commercially available graphene ink on to the surface of the e-jet printed elastomers, which builds on previous work in printed sensors for soft robotics through greater conductivity.^[15]

In AJ, a functional ink is atomized, suspended within a carrier gas, and directed at a substrate that can then be articulated with respect to the deposition head to achieve spatial patterning. By combining an effective focusing mechanism with the production of uniform aerosol, AJ can produce deposits with resolutions approaching 20 μm .

For AJ, a Collison atomizer was used to produce the aerosol from the bulk ink. Residual pressure drives the aerosol from the atomization chamber, through a virtual impactor, and towards the deposition head. The virtual impactor refines the aerosol by removing droplets with insufficient inertia to be impacted on the substrate. At the deposition head, the aerosol is focused by introducing an annular sheath gas in combination with a physical nozzle (Figure 2a). As such, controlling the geometry of AJ printed features requires consideration of the nozzle speed and geometry, relative gas flow rates (focusing ratio), and the evaporation characteristics of the ink.

Deposition from nozzle heights of 1–3 mm produced consistent features with a moderate focal point at $\approx 2 \text{ mm}$ (Figure 2b). From distances of 3–8 mm, the maximum height of printed traces decreased from 0.25 to 0.05 μm and the FWHM increased from $\approx 100 \mu\text{m}$ to over 450 μm ; therefore, showing a loss of aerosol jet collimation at elevated print heights. The quality ratio, a comparison between the subjective maximum width of the line and the FWHM (Figure S4–S6, Supporting Information), supports this since deposition at 1 mm reliably produced the highest quality features.

Increasing nozzle velocity led to small changes to the width and height (Figure 2c) that can be attributed to the normal distribution of droplets in the aerosol stream leading to increased height growth at the center of the line when compared to the edges. At high print speeds, the maximum height of the line is comparable to the magnitude of overspray, therefore the line quality appears higher as the FWHM approaches the maximum line width.

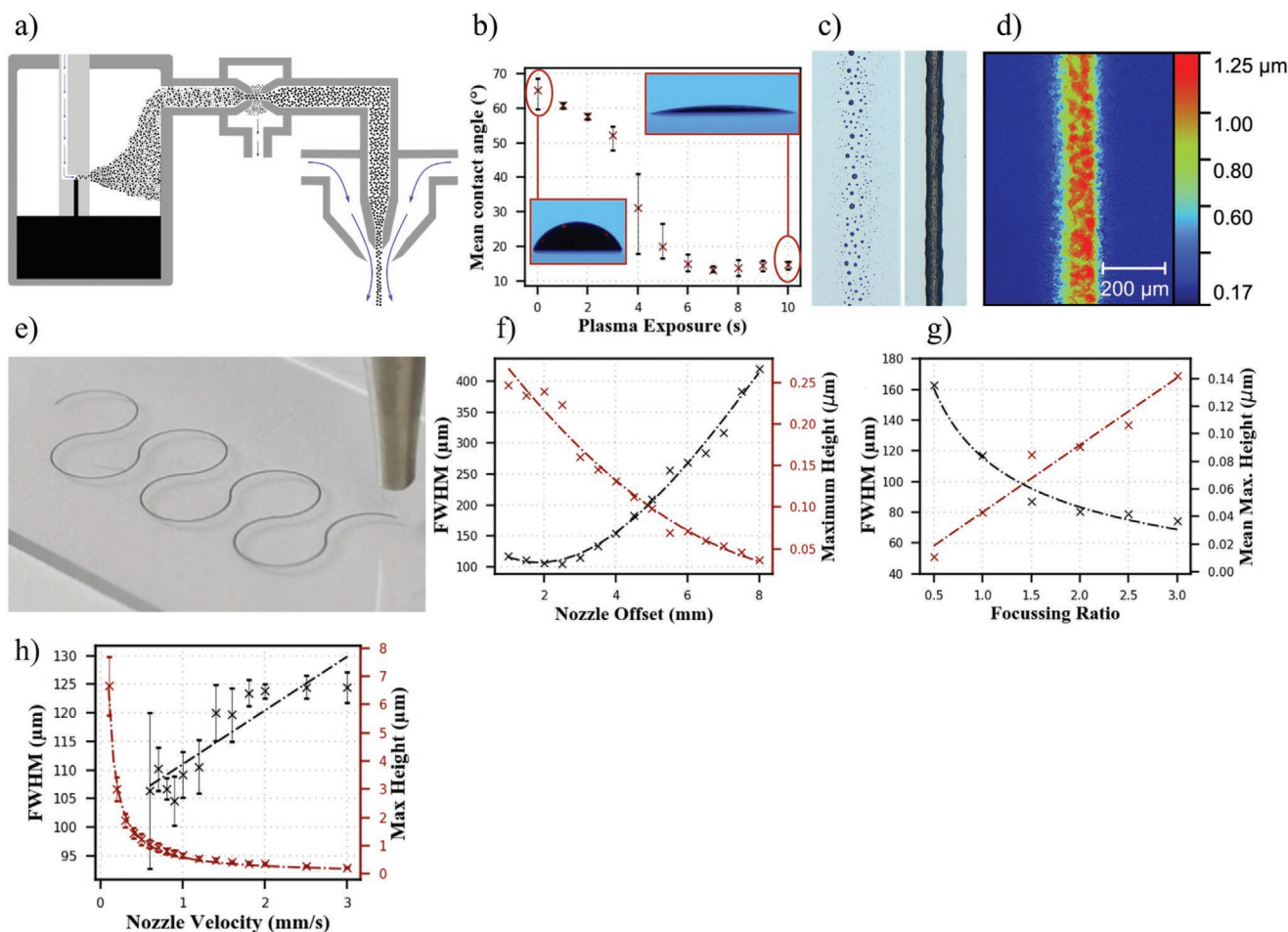


Figure 2. a) Schematic of the aerosol jet process, b) effect of oxygen plasma exposure time on the contact angle between graphene ink and PDMS, c) printed feature on PDMS before and after plasma treatment, d) surface profile of a AJ printed trace, e) image of AJ deposition on glass, f–h) the effect of nozzle offset, focussing ratio, and nozzle velocity on the full width at half maximum height (FWHM) and peak feature height, respectively.

The focusing ratio, defined as the ratio of the sheath gas flow to the atomizer flow, was found to have the inverse relationship to the nozzle height and velocity (Figure 2f). Through manipulation of the focusing ratio, the FWHM and line height could be varied from 50–160 μm and 0.01–0.14 μm , respectively.

For conductive traces, high aspect ratio features are typically targeted as they allow low resistivity at greater trace densities. This is more evident in stretchable conductive sensors as the aspect ratio has a direct effect on the stress present in serpentine, patterned stretchable features. As can be seen in **Figure 3**, the print process should target low-velocity, high focusing ratio, and moderate-to-low stand-off heights within a processing window that produces sufficient line quality (Figure S4–S6, Supporting Information).

Our previous work has shown how high-strain could be achieved at the expense of conductivity.^[15] The use of a graphene nanoplatelet ink provides significantly greater conductivity ($62.6 \Omega \text{ sq}^{-1}$) at the expense of strain tolerance. Through considered design, stress can be minimized to enable moderate strains from relatively stiff electrode material.

The production of free-standing soft films required separation of the PDMS-graphene structure from the underlying

substrate. This introduced additional challenges due to tearing or deformation of the films. For soft films, this is particularly challenging as they have low tensile strength when compared to rigid polymer or metallic materials. Simple mechanical removal was found to tear films, especially when separating thin devices that consisted of a low number of layers. To overcome this, a thin sacrificial layer (<1 μm) of polyvinyl-alcohol was spin coated on to the substrates prior to deposition. This layer could then be dissolved in a heated ultrasonic bath following printing to release the film.

Combining the sacrificial support with E-Jet printing, plasma treatment, and aerosol jet printing to produce a single device creates opportunities for soft films with integrated functionality. A proof-of-concept, five-layer structure consisting of three layers of PDMS with two electrode layers was produced (Figure 3). With electrode and PDMS layers of 3 and 65 μm , respectively, the final thickness of the device was approximately 200 μm and had a surface roughness of $\approx 0.26 \mu\text{m}$ (S_a) measured over a 2 mm^2 surface area. In this particular early demonstrator, the surface roughness was impacted by atmospheric dust ingress during manufacture, while higher film thicknesses were targeted for improved process reliability at this experimental

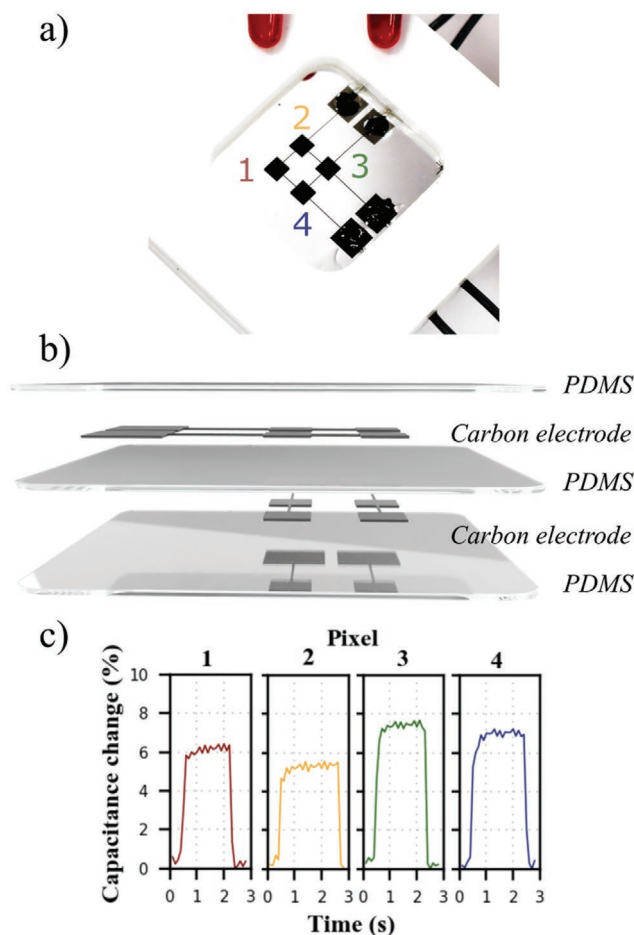


Figure 3. a) Five-layer, four-pixel printed sensor mounted within an acrylic frame, b) CAD explosion of the sensor design, and c) response of each pixel in response to touch.

stage. Electrical connection was made using a carbon grease in combination with cyanoacrylate for strain relief. This resulted in a four-pixel capacitive sensor that exhibited a 5–8% change in response upon touch. Subjectively, limited strain tolerance was observed in these early devices, however on-going research to quantify the response, improve materials, and evaluate application specific performance is being enabled by the process and will form the basis of future communications. Although conceptually simple, this first demonstrator shows the value in an integrated, hybrid, and digitally driven approach that is tolerant of inks with disparate rheology for the manufacture of functional soft devices.

We present a new approach that combines alternating current electro-hydrodynamic deposition of high viscosity, low-conductivity elastomer films with aerosol direct write of conductive traces to overcome rheological constraints of the respective processes. Using electrically forced jets, this approach overcomes challenges in nozzle blocking usually associated with the direct write of thin elastomeric films. Droplet sizes of approximately 800 pL were achieved during this work resulting in feature thicknesses of 5 μm using a 160 μm ID nozzle. Reduction of the nozzle diameter, and improved control of the material flow, presents a pathway to higher resolution patterning. By

integrating a complimentary direct write technique with EHD, we demonstrate a digitally driven, hybrid manufacturing process that enables the automated manufacture of soft, functional film-based devices.

Experimental Section

Substrate Preparation: Square substrates (50 \times 50 mm) were prepared from 300 \times 300 sheets of 125 μm polyethylene terephthalate (PET) (Goodfellow, UK). Polyvinyl alcohol (PVA, MP Biomedicals) mixed with deionised water at 3 wt% and left to stir for at least 48 h. A layer was then spin coated on to the PVA sheets at 500 RPM for 60 s. Dissolution was achieved by leaving the printed structures in an ultrasonic bath at 80 $^{\circ}\text{C}$.

Electrohydrodynamic Printing: The silicone elastomer, Sylgard 1-4128 (Dow Corning, USA), was prepared by mixing part A and B in a ratio of 10:1 in a planetary mixer degasser (Thinky ARE-310, Intertronics, UK). This variant of Sylgard was selected for its long pot life and rapid curing at elevated temperatures. Once prepared, the material was loaded in to a ten milliliter syringe and secured in to a syringe pump (Harvard Precision Instruments, USA). Using luer-lock connections, the syringe was attached to a 30-gauge (OD: 310 μm , ID: 160 μm) stainless steel blunt nozzle by a length of Tygon tubing. The nozzle was then mounted to the deposition head before deposition. Voltage was applied to the nozzle using a high voltage amplifier (20/20C-HS, Trek, USA) in combination with a function generator (AFG2021, Tektronix, USA). PDMS was cured using a hot plate at 105 $^{\circ}\text{C}$ for 5 min. All deposition was conducted on bespoke apparatus designed and constructed for this work. Post-print, nozzles were flushed using ethyl acetate and deionized water to remove any remaining material. Blocked nozzles were cleared through mechanical removal with fine gauge needles.

Aerosol Jet Printing: Samples were exposed to a bulk oxygen plasma treatment for six seconds to increase wettability (Plasma Etch, USA). They were then mounted to a deposition stage (Thorlabs, USA) heated to 120 $^{\circ}\text{C}$ to encourage solvent evaporation. 50 mL of a commercially available graphene nanoplatelet ink (500 nm platelets in an aqueous suspension with \approx 1% PEDOT:PSS, viscosity: 10 cP) (CAMINK IJ3, Cambridge Nanosystems, UK) was loaded in to the pneumatic atomizer, held at 30 $^{\circ}\text{C}$, and stirred continuously at 200 rpm. Three layers were aerosol jet printed (Optomec, USA) for each electrode to improve conductivity. Flow rates of 400 and 200 sccm were used for the atomizer and sheath, respectively. Substrate actuation was conducted on bespoke apparatus.

Metrology: 3D measurements of elastomer droplets and printed electrodes were acquired using white light interferometry (NP Flex, Bruker, USA). This data was used to determine the volume and contact angle of deposits. Four cross sections were taken and an average used to determine the contact angle (Figure S1, Supporting Information). Since no solvents were used, and PDMS had a low shrinkage (\approx 1%), the droplets were assumed to have approximately equal values to the deposit. For AJ printed traces, the full width at half maximum was used as an objective measure of track width. Optical microscopy (Olympus BX53M) was used for 2D measurements. Conductivity of samples was measured using four-point probing (Jandel, UK). Contact angle measurements of the conductive graphene platelet ink on PDMS substrates were taken using a goniometer (Ossila, UK) through the sessile drop technique. This approach was used over white light since the contact angles were much larger and more prone to variance over time due to solvent evaporation.

Capacitive Sensing: Connections to the sensor were achieved using carbon grease (MG Chemicals, USA), in combination with an acrylic frame and cyanoacrylate (3M, UK) for strain relief. A thicker layer of PDMS was cast before removal from the PET film to protect the sensor an increase mechanical robustness. Measurements were taken using a capacitance-to-digital converter development board (AD7746, Analog Devices, USA) and verified using a calibrated multimeter (Keithley

2110, USA). Since the development board had a single input, pixel selection and cycling was achieved by combining an Arduino Mega with a multiplexer (CD74HC4067, Sparkfun, USA). This approach allowed readings to be taken with a frequency ≈ 100 Hz.

Supporting Information

Supporting Information is available from the Wiley Online Library or from the author.

Acknowledgements

The authors kindly acknowledge the support of the Engineering and Physical Sciences Research Council (EPSRC) through grants EP/M026388/1, EP/L02067X/2, and EP/P027687/1.

Conflict of Interest

The authors declare no conflict of interest.

Keywords

aerosol jet, fabrication, hybrid manufacturing, soft robotics

Received: February 21, 2020

Revised: March 19, 2020

Published online: May 4, 2020

- [1] M. Cianchetti, C. Laschi, A. Menciassi, P. Dario, *Nat. Rev. Mater.* **2018**, *3*, 143.
- [2] H. Zhao, A. M. Hussain, A. Israr, D. M. Vogt, M. Duduta, D. R. Clarke, R. J. Wood, *Soft Robot.* **2020**, <https://doi.org/10.1089/soro.2019.0113>.
- [3] M. Imboden, E. de Coulon, A. Poulin, C. Dellenbach, S. Rosset, H. Shea, S. Rohr, *Nat. Commun.* **2019**, *10*, 834.
- [4] A. Atalay, V. Sanchez, O. Atalay, D. M. Vogt, F. Haufe, R. J. Wood, C. J. Walsh, *Adv. Mater. Technol.* **2017**, *2*, 1700136.
- [5] K. Xu, Y. Lu, K. Takei, *Adv. Mater. Technol.* **2019**, *4*, 1800628.
- [6] S. Rosset, H. R. Shea, *Appl. Phys. Rev.* **2016**, *3*, 031105
- [7] P. Lotz, M. Matysek, H. F. Schlaak, *IEEE/ASME Trans. Mechatronics* **2011**, *16*, 58.
- [8] H. Zhao, A. M. Hussain, M. Duduta, D. M. Vogt, R. J. Wood, D. R. Clarke, *Adv. Funct. Mater.* **2018**, *28*, 1804328.
- [9] S. Rosset, O. A. Ararom, S. Schlatter, H. R. Shea, *J. Visualized Exp.* **2016**, *108*, 53423.
- [10] A. Poulin, S. Rosset, H. R. Shea, *Appl. Phys. Lett.* **2015**, *107*, 244104.
- [11] F. M. Weiss, T. Töpfer, B. Osmani, S. Peters, G. Kovacs, B. Müller, *Adv. Electron. Mater.* **2016**, *2*, 1500476.
- [12] R. L. Truby, M. Wehner, A. K. Grosskopf, D. M. Vogt, S. G. M. Uzel, R. J. Wood, J. A. Lewis, *Adv. Mater.* **2018**, *30*, 1706383.
- [13] D. McCoull, S. Rosset, S. Schlatter, H. Shea, *Smart Mater. Struct.* **2017**, *26*, 125022.
- [14] A. D. Valentine, T. A. Busbee, J. W. Boley, J. R. Raney, A. Chortos, A. Kotikian, J. D. Berrigan, M. F. Durstock, J. A. Lewis, *Adv. Mater.* **2017**, *29*, 1703817.
- [15] N. J. Wilkinson, M. Lukic-Mann, M. P. Shuttleworth, R. W. Kay, R. A. Harris, in *2019 2nd IEEE Int. Conf. on Soft Robotics (RoboSoft)*, IEEE, Seoul, Korea (South) **2019**, pp. 496–501.
- [16] E. Bihar, T. Roberts, E. Ismailova, M. Saadaoui, M. Isik, A. Sanchez-Sanchez, D. Mecerreyes, T. Hervé, J. B. De Graaf, G. G. Malliaras, *Adv. Mater. Technol.* **2017**, *2*, 1600251.
- [17] M. S. Onses, E. Sutanto, P. M. Ferreira, A. G. Alleyne, J. A. Rogers, *Small* **2015**, *11*, 4237.
- [18] J.-U. Park, M. Hardy, S. J. Kang, K. Barton, K. Adair, D. K. Mukhopadhyay, C. Y. Lee, M. S. Strano, A. G. Alleyne, J. G. Georgiadis, P. M. Ferreira, J. A. Rogers, *Nat. Mater.* **2007**, *6*, 782.
- [19] A. Lee, H. Jin, H. W. Dang, K. H. Choi, K. H. Ahn, *Langmuir* **2013**, *29*, 13630.
- [20] J. Xue, J. Xie, W. Liu, Y. Xia, *Acc. Chem. Res.* **2017**, *50*, 1976.
- [21] A. Jaworek, A. T. Sobczyk, A. Krupa, A. Marchewicz, A. K. Krella, T. Czech, *Int. J. Plasma Environ. Sci. Technol.* **2016**, *10*, 29.
- [22] S. N. Jayasinghe, M. J. Edirisinghe, *J. Aerosol Sci.* **2004**, *35*, 233.
- [23] S. N. Jayasinghe, M. J. Edirisinghe, *Appl. Phys. Lett.* **2004**, *85*, 4243.
- [24] F. M. Weiss, T. Töpfer, B. Osmani, H. Deyhle, G. Kovacs, B. Müller, *Langmuir* **2016**, *32*, 3276.
- [25] L.-F. Ren, F. Xia, J. Shao, X. Zhang, J. Li, *Desalination* **2017**, *404*, 155.
- [26] Y.-L. Sung, J. Jeang, C.-H. Lee, W.-C. Shih, *J. Biomed. Opt.* **2015**, *20*, 047005.
- [27] E. B. Secor, *Flexible Printed Electron.* **2018**, *3*, 035002.
- [28] N. J. Wilkinson, M. A. A. Smith, R. W. Kay, R. A. Harris, *Int. J. Adv. Manuf. Technol.* **2019**, *105*, 4599.